

## Supporting Information

# Anthracene-bisphosphonate based novel fluorescent organic nanoparticles explored as apoptosis inducer of cancer cells

Malay Pramanik,<sup>a</sup> Nabanita Chatterjee,<sup>b</sup> Subhadip Das,<sup>b</sup> Krishna Das Saha\*<sup>b</sup> and  
Asim Bhaumik\*<sup>a</sup>

<sup>a</sup>Department of Materials Science, Indian Association for the Cultivation of Science, Jadavpur, Kolkata-  
700 032, INDIA

<sup>b</sup>Cancer Biology and Inflammatory Disorder Division, CSIR-Indian Institute of Chemical Biology,  
Jadavpur, Kolkata- 700 032, INDIA

### Table of contents

Section S1	Synthesis procedure of TEABP [C <sub>22</sub> H <sub>28</sub> O <sub>6</sub> P <sub>2</sub> ]	Page 2
Section S2	<sup>1</sup> H, <sup>13</sup> C, <sup>31</sup> P and MAS spectra of TEABP	Page 3-4
Section S3	Wide-angle X-ray diffraction pattern and minimal energy structure of TEABP	Page 5
Section S4	Photophysical and biological experimental section(s)	Page 5-12
Section S5	Characterization techniques	Page 13
Section S6	Photophysical property of TEABP	Page 13-14
Section S7	Solid state optical property OF TEABP FON	Page 14-15
Section S8	Emission spectrum of TEABP	Page 15-17
Section S9	ICT VS intermolecular aggregation	Page 17-18
Section S10	SEM image of TEAB	Page 18
Section S11	Time resolved spectroscopy	Page 19-20
Section S12	pH dependent emission study of TEABP	Page 20-22
Section S13	Emission study of TEABP FON in water	Page 22
Section S14	Bond lengths and bond angles of minimal energy structure of TEABP	Page 23-25
Reference	Reference 1-19	Page 25-26

## **Section S1: Synthesis procedure of TEABP**

### **Materials**

Commercially available 9,10-dibromo-anthracene (98 %), triethyl phosphite (98 %) and 1,3-diisopropyl benzene were purchased from Sigma-Aldrich. Anhydrous nickel (II) bromide (99 %) was purchased from Avra-chemical. The spectroscopic grade solvents (hexane, chloroform, DMF, DMSO, methanol) were purchased from E-Merck.

**Synthesis of tetraethyl anthracene-9,10-diyl-9,10-bis(phosphonate) [C<sub>22</sub>H<sub>28</sub>O<sub>6</sub>P<sub>2</sub>]** We have synthesized tetraethyl anthracene-9,10-diyl-9,10-bis(phosphonate) (TEABP) by slight modification over classical Arbuzov reaction. 9,10-dibromo-anthracene (3.36 gm, 10 mmol) was dissolved into 30 ml 1,3-diisopropyl benzene and heated at 150 °C in a three necked 100 ml round bottom flask fitted with a water cooled condenser, N<sub>2</sub> inlet and an additional airtight funnel. After 30 min of heating the round bottom flask was cooled to 120 °C and 0.50 gm anhydrous nickel (II) bromide was added to the greenish yellow solution. The flask was now heated to 185°C and 8 ml triethyl phosphite was added to the solution over 3 h period under gentle stream of N<sub>2</sub>. The mixture was refluxed for another 6 h in inert atmosphere and finally a bluish-black solution was distilled under vacuum to remove the solvent and unreacted triethyl phosphite. The bluish-black viscous material was purified over column chromatography. The compound was eluted with a mixture of chloroform and hexane in a composition of 70:30 (V/V). Vacuum evaporation of the highly blue fluorescent elutant produced the blue solid compound. The yield was 1.71 g (37 %). The compound was characterized by <sup>1</sup>H, <sup>13</sup>C, <sup>31</sup>P NMR, IR, and MAS spectroscopy. We have collected the TEABP FON by re-dissolving the product in water/ethanol [20:1 (v/v)] mixture and re-precipitate from the mixture solvent. The compound was dried under high vacuum pump and preserved in vacuum desiccator.

## Section S2: $^1\text{H}$ , $^{13}\text{C}$ , $^{31}\text{P}$ and MAS spectra of TEABP

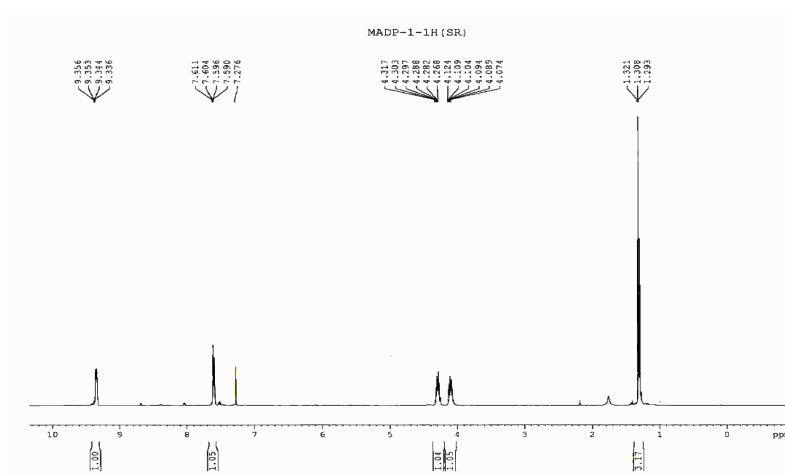


Figure S1.  $^1\text{H}$  NMR spectrum of TEABP

$^1\text{H}$  NMR (500 MHz,  $\text{CDCl}_3$ )  $\delta$  = 9.33–9.35 (dd, 4H,  $J_1$  = 1.5 Hz,  $J_2$  = 7.5 Hz); 7.59–7.61 (dd, 4H,  $J_1$  = 3 Hz,  $J_2$  = 7.25 Hz); 4.26–4.31 (m, 4H); 4.07–4.12 (m, 4H); 1.30 (t, 12H,  $J$  = 6.5 Hz).

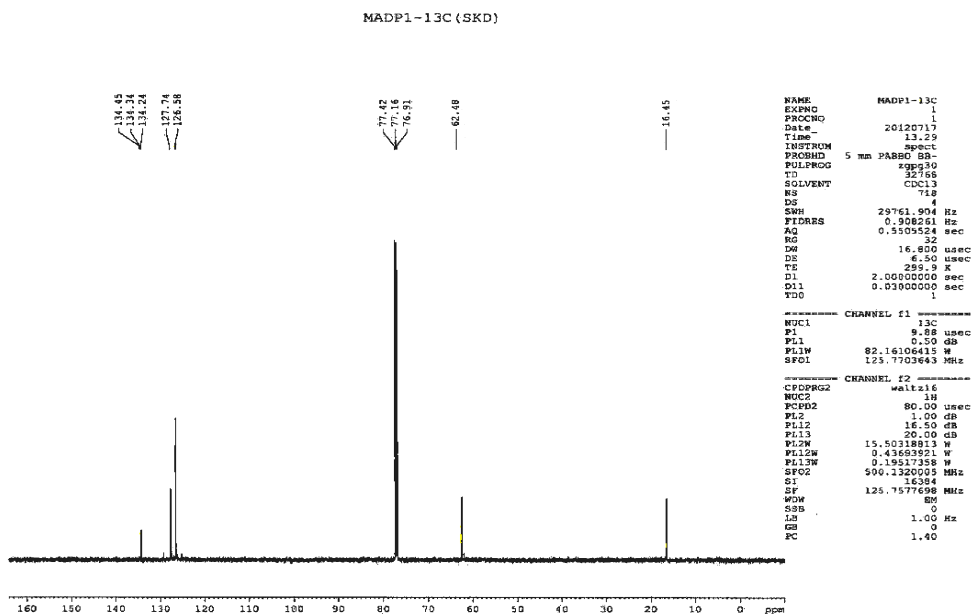


Figure S2.  $^{13}\text{C}$  NMR spectrum of TEABP

$^{13}\text{C}$  NMR (500 MHz,  $\text{CDCl}_3$ )  $\delta = 16.45, 62.48, 126.58, 127.74, 134.24, 134.34, 134.45$ .

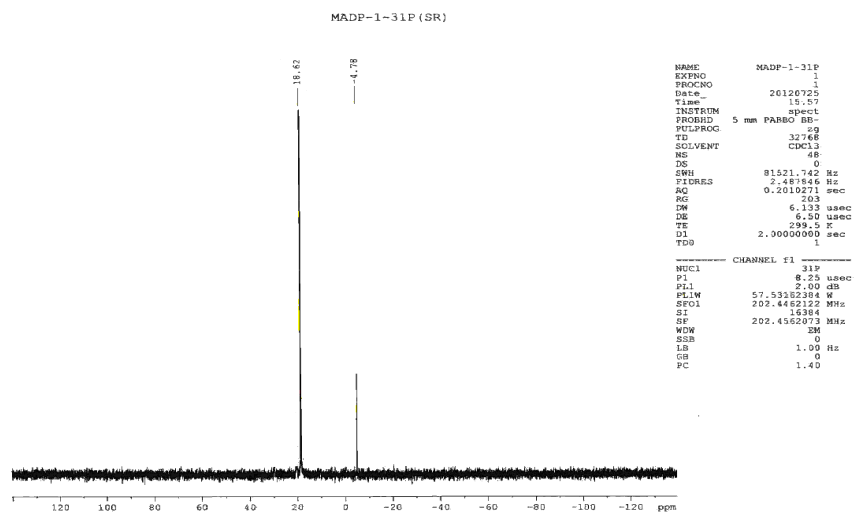


Figure S3.  $^{31}\text{P}$  NMR spectrum of TEABP

$^{31}\text{P}$  NMR (500 MHz,  $\text{CDCl}_3$ ,  $\text{PPh}_3$  was used as the standard material)  $^{31}\text{P} = 18.62$

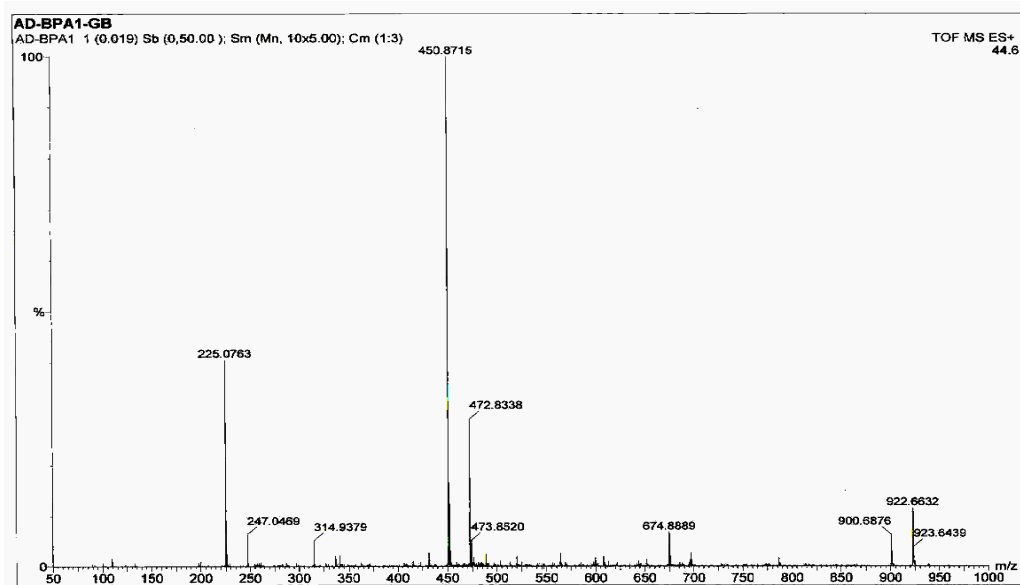
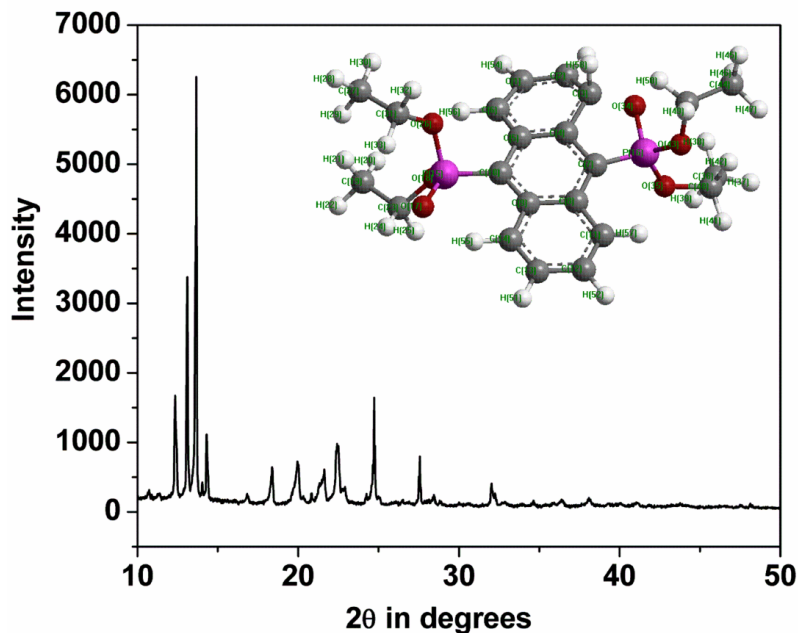


Figure S4. MAS spectrum of TEABP MS (EI):  $m/z$ : 450.8715 ( $\text{M}^+$ ).

### Section S3: Wide-angle X-ray diffraction pattern and minimal energy structure of TEABP



**Figure S5.** X-ray diffraction pattern and minimal energy structure of TEABP  
The energy minima structure of the molecule (TEABP) (inset of Figure S1) has been evaluated by MOPAC-2012 and the corresponding bond distance and bond angles are listed below.

### Section S4: Photophysical and biological experimental section

**(a) Photophysical measurements.** The steady state electronic adsorption and emission spectra of TEABP were recorded in different solvents with varying polarity ( $\epsilon = 0$  to 80) on Cary Varian 50 scan UV-Vis optical spectrometer equipped with 'Cary Win' UV software 6.7. The concentrations of the solutions were  $1.04 \times 10^{-7}$  mole  $\text{dm}^{-3}$ . Fluorescence studies of the solutions were carried out in a Perkin Elmer LS55 Fluorescence spectrometer instrument. The solution was kept in a quartz cell of 1 cm path length and excited at 265 nm and emission spectra were recorded from 280-600 nm using a slit width of 2.5 nm. All the measurements were carried out at an ambient temperature of 298K.

**(b) Time Resolved Measurements.** The life-times of the organic fluorphore (TEABP) in different solvents were measured by time correlated single photon counting (TCSPC) technique in a HORIBA JOBIN YVON instrument. The system was excited at 280 nm by using picoseconds diode laser (IBH Nanoled-07). The detector was a Hamamatsu MCP plate photomultiplier (R3809U). The single photon counting technique comprised an Ortec 9327

discriminator (CFD, Tenelec TC 454) and Fluoro Hub Single Photon Counting controller. The data were collected by a DAQ card as a multichannel analyzer. The spectra obtained were analyzed by using the Software DAS6 at Data Stationv2.3 through exponential fitting of the corresponding lifetimes. The quality of fitting was measured by reduced  $\chi^2$  values.

### **(c) Cell culture**

Human leukemic monocyte lymphoma cells (U937 cells), Human Hepatocellular carcinoma (HepG2 cells), Human colorectal carcinoma cells (HCT 116 cells), Human cervical adenocarcinoma cells (HeLa cells), Human breast adenocarcinoma cells (MCF7 cells) and Human lung carcinoma cells (A549 cells) [American Type Culture Collection, ATCC] were used. The cells were cultured in RPMI or DMEM supplemented with 10% fetal bovine serum (FBS) and 1% antibiotic (PSN) at 37°C in a humidified atmosphere under 5% CO<sub>2</sub>. After 75-80% confluency, cells were harvested with 0.025% trypsin and 0.52 mM EDTA in phosphate buffered saline (PBS) (for adherent cells), and seeded at desired density to allow them to re-equilibrate a day before the start of experiment.

### **(d) MTT assay**

MTT assay was done to evaluate cell viability. The cells were plated in 96 well plates and treated with or without different concentrations of TEABP for 24 h. Four hours after the addition of MTT, cells were lysed and formazan was solubilized with acidic isopropanol and the absorbance of the solution was measured at 595 nm using an ELISA reader.<sup>1</sup>

Treatment of TEABP ranging concentration from 0 to 30  $\mu$ M on a panel of six human cancer cell lines of different origins, namely, U937, HepG2, HCT116, HeLa, MCF7, and A549 for 24 h showed various degree of cell death as shown in Fig.S4(d). IC<sub>50</sub> values of the compounds on 24 h on these cell lines were shown in the S4(d-2). Optimum and significant cell death on U937 cells was near about 90% in 24 h with 30  $\mu$ M of TEABP and then we selected the concentration 15  $\mu$ M of TEABP as experimental concentration for other biological studies.

However, TEABP did not show any cytotoxic effect on peripheral blood mononuclear cells (PBMC) as we found from cytotoxicity study given in Fig. S4(d-1).

### Section S4(d): MTT of TEABP on different cancer cells

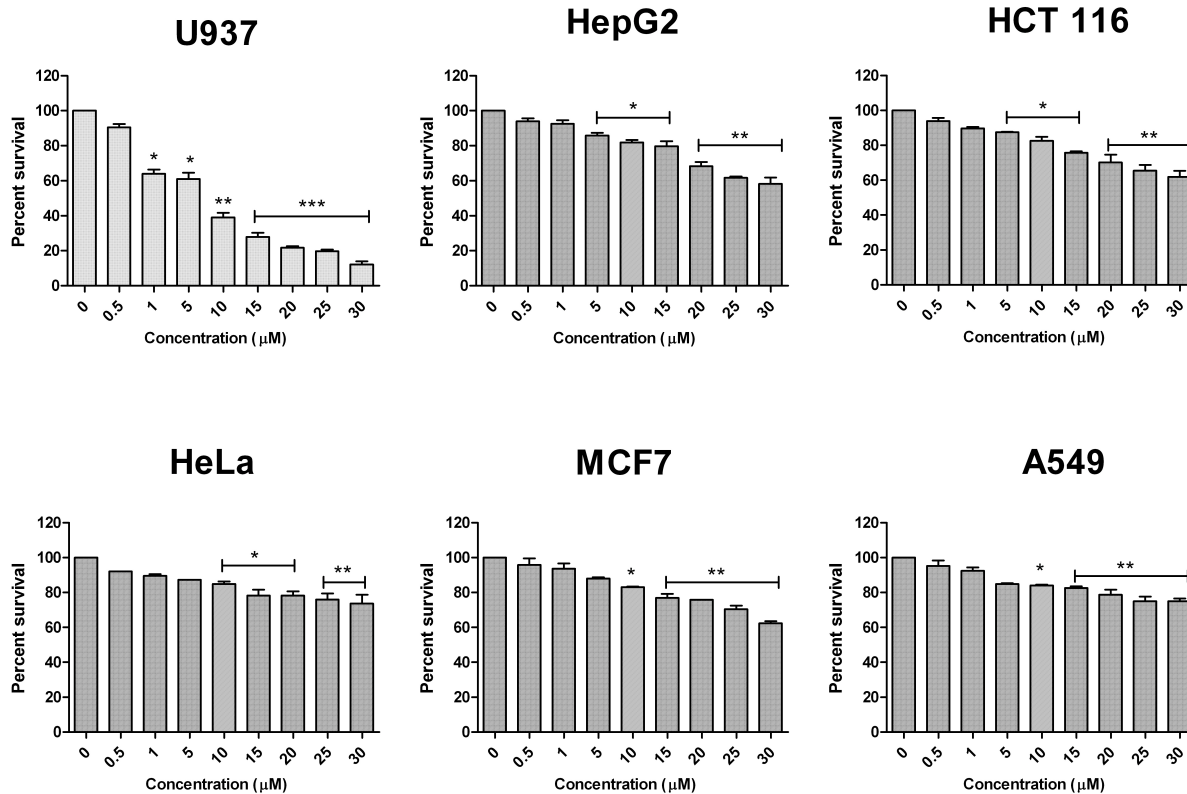


**Figure S4(d).** Growth inhibitory effect of fluorescent organic nanoparticles (FONs), tetraethyl anthracen-9, 10-diyl-9, 10-bis (phosphonate) [TEABP] on different cancer cells. on U937, HepG2, HCT116, HeLa, MCF7, and A549. Cells were treated with different concentrations (0, 0.5, 1, 10, 15, 20, 25, 30 μM) of the TEABP for 24 h and viability was measured by MTT assay. The data are represented as mean ± SEM (\*P<0.05, \*\*P<0.01) of triplicate independent experiments.

**Section S4(d-1): Cytotoxicity of TEABP on peripheral blood mononuclear cells:**

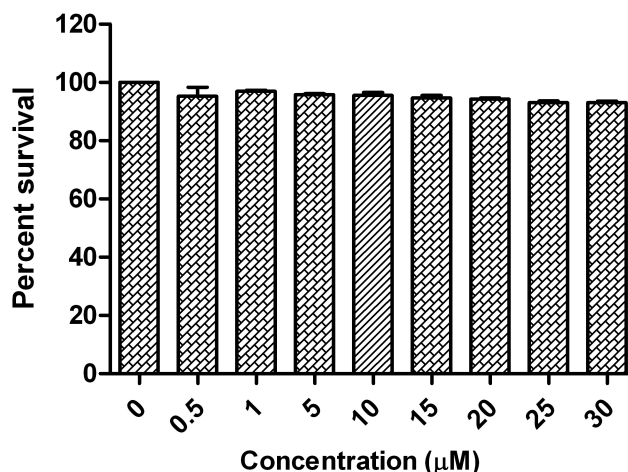


**Figure S4(d-1).** Cytotoxic effect of fluorescent organic nanoparticles (FONs), tetraethyl anthracen-9, 10-diyl-9, 10-bis (phosphonate) [TEABP] on peripheral blood mononuclear cells (PBMC): Cells were treated with different concentrations (0, 0.5, 1, 10, 15, 20, 25, 30µM) of the TEABP for 24 h and viability was measured by MTT assay. The data are represented as mean  $\pm$  SEM from triplicate independent experiments. No significant change was found.

**Section S4(d-2): IC<sub>50</sub> values of TEABP on different cancer cells :**

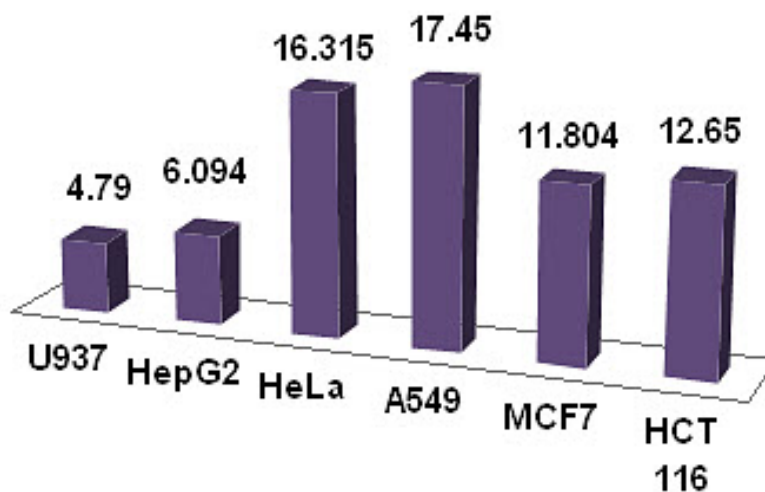


**Figure S4(d-2).** IC<sub>50</sub> values of TEABP in different cell lines. The TEABP was treated with 0, 0.5, 1, 10, 15, 20, 25, 30 µM on U937, HepG2, HeLa, A549, MCF7 and HCT116 for 24 h. MTT assay was performed to calculate IC<sub>50</sub> values. Values are mean of at least three different experiments and errors represent S.E.M. values.

**(e) Assessment of cellular morphology and Fluorescence microscopy**

Cells ( $1 \times 10^4$ /well) grown in 6-well plates in RPMI supplemented with 10% FBS for 24 h were treated with or without compound. Morphological changes were observed with an inverted phase contrast microscope (Model: OLYMPUS IX 70, Olympus Optical Co. Ltd.) and images were acquired. For the detection of nuclear damage or chromatin condensation, treated and untreated cells were stained with 10  $\mu\text{g/ml}$  of DAPI.<sup>2</sup> Cells were stained with AO/Et.Br in order to distinguish the live, apoptotic and necrotic ones, and observed under fluorescence microscope; images were then acquired with excitation and emission wavelengths of 488 and 550 nm respectively.<sup>3</sup>

**(f) Quantification of apoptosis using Annexin-V**

Apoptosis was assayed by using an Annexin-V FITC apoptosis detection kit (Calbiochem, CA, USA). Briefly, cells were treated with or without derivatives, then washed and stained with PI and Annexin-V-FITC in accordance with the manufacturer's instructions. The percentages of live, apoptotic and necrotic cells were determined by flow cytometric method (Beckton Dickinson, San Jose, CA, USA). Data from  $10^6$  cells were analyzed for each sample.

**(g) Cell cycle analysis**

U937 cells were seeded in 6-well plates and treated with TEABP. Harvested cells were fixed over-night in 70% ethanol at 4°C, collected by centrifugation, resuspended in phosphate-buffered saline (PBS) containing 25  $\mu\text{g/ml}$  RNase and 0.5% Triton-X100, and incubated for 1 h at 37°C. Cells were stained with 50  $\mu\text{g/ml}$  PI for 15 min at 4°C and analysed by flow cytometer ( $10^4$  cells were counted).

### Section S4(g): Cell cycle analysis of TEABP on U937 cells:

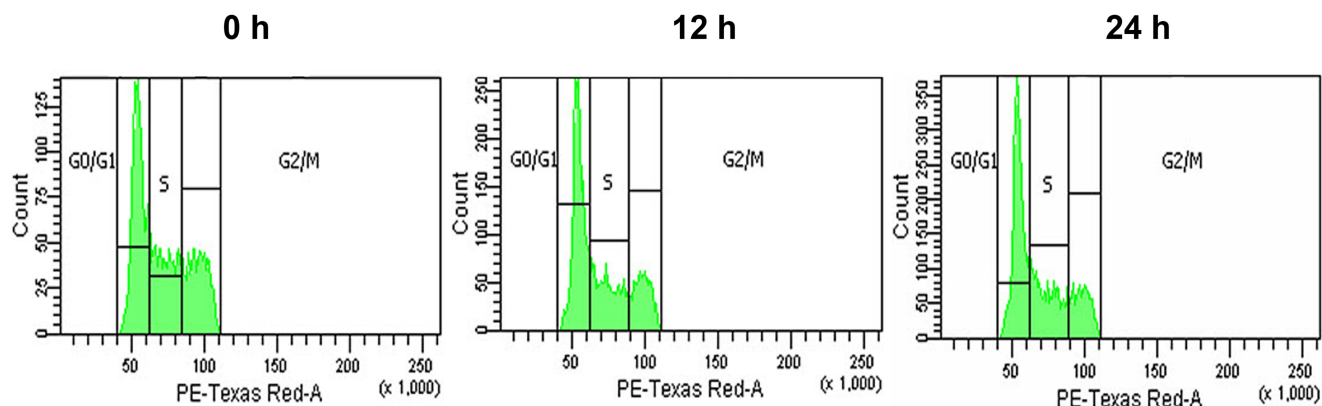


**Figure S4(g). Study of cell cycle arrest in U937 cells by propidium iodide:** Cell cycle consisting of four regulations phases (G0/G1, S, G2, and M), is an integrated part of cell growth. Apoptosis is followed by cell cycle arrest at any one of these phases. So, status of cell cycle arrest in TEABP treated U937 cells were monitored by Flow cytometric analysis using PI. Treatment of 15  $\mu\text{M}$  of TEABP for 12h and 24 h showed higher percent of cells at G0/G1 phase. This study indicated that the active compound TEABP induced apoptosis of U937 cells through cell cycle arrest at G1/S phase.

#### **(h) Western blot analysis**

The cell lysates were separated by 10% SDS-PAGE then transferred to PVDF membranes (Millipore, Bedford, MA) using standard electroblotting procedures. Membranes were then blocked and immunolabeled overnight at 4°C with primary antibodies. Alkaline phosphatase conjugated secondary antibodies and NBT-BCIP were used as chromogenic substrates.

Western blot analysis revealed that the treatment of U937 cells with TEABP at the concentration of 15  $\mu\text{M}$  for 24 h lowered the levels of Bcl-2 and Bcl-XL whereas level of Bax, and p53 were increased (Fig. S4 h).

### Section S4(h): Western blot analysis of TEABP on U937 cells

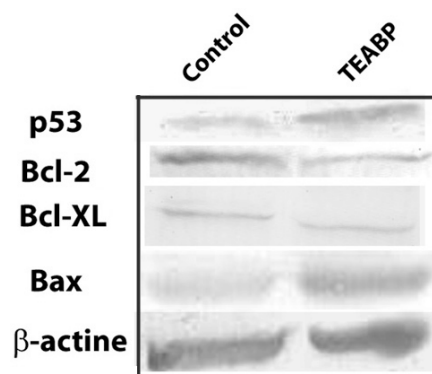


**Figure S4(h): Western blot analysis of TEABP on U937 cells:** Western Blot analyses of some important pro- and anti-apoptotic proteins in treated and untreated U937 cells. Cells were treated with 15  $\mu$ M of TEABP for 24 h. Cells were lysed and cell lysate were used for Western Blot Analysis. Panel represents western blot analysis of different apoptotic marker proteins indicates P53, Bcl2, Bcl-XL and Bax with  $\beta$ -Actin expression after 15  $\mu$ M of TEABP for 24 h.

#### **(i) In vitro cell imaging and cellular uptake studies**

Moreover, fluorescence imaging confocal scanning microscopy is an indispensable tool to gain the precisely visual evidence relating apoptosis initiation and its optophysical property. As shown in figure 3 the cell morphology remains unaltered and no characteristic changes are detected in untreated cell with TEABP. Whereas the cell treated with fluorescent organic nanoparticle (TEABP) exhibit obvious morphological changes including the cytoplasmic blebbing, which confirms the successful induction of apoptosis. It is easily observed in the cell treated with a TEABP, which emits bright blue fluorescence in contrast to the untreated cells.

Cell imaging studies was carried out using the U937 cell line which was maintained proper cell culture condition. To study the cellular uptake of the compound TEABP, cells ( $1 \times 10^4$ /well) were grown on 30 mm Petri dish well plates for 24 h at 37  $^{\circ}$ C and 5% CO<sub>2</sub> followed by incubation with TEABP in cell culture medium for 12 h. Cells were washed three times with PBS and fixed by paraformaldehyde subject to imaging by confocal laser scanning microscope (Nikon A1R) using the respective filter. Cellular uptake study after 12 h incubation reveals that TEABP is internalized by the cell membrane leading to a uniform distribution inside the cell.

Cellular uptake experiments were conducted according to a literature method with some modifications. U937 cells ( $3 \times 10^4$  cells) were seeded in 60 mm tissue culture dishes containing culture medium (2 ml/well) and incubated at 37 °C in an atmosphere of 5% CO<sub>2</sub>/95% air for 24 h.

After exposure to 15 μM of TEABP for 3, 6, and 12 h, the cells were taken and washed 4 times with ice-cold PBS. Cells then were suspended in 1 ml of PBS and applied to the FACS analyzer (BD LSRFortessa) for uptake study.

#### Section S4(i): Cellular uptake study of TEABP on U937 cells:

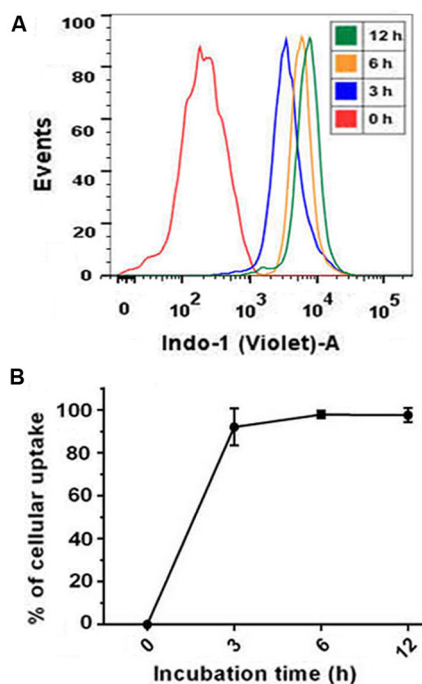


**Figure S4(i). Cellular uptake studies: % cellular uptake of TEABP by U937 cells with increasing time (h).** Cellular uptake studies were also performed to ascertain whether the cytotoxicity results correlated with the cellular levels. The accumulation of TEABP was confirmed by (A) FACS analysis of cellular dye uptake using U937 cells. The uptake level was found at 15 μM of TEABP with time-dependently up to 12 h. Notably, the uptake was found to be linear at first six hours and then became plateau till 12<sup>th</sup> hour (with respect to time) as represent graphically in (B).

### **Section S5: Characterization techniques**

A Jeol JEM 6700 field emission scanning electron microscope (FE-SEM) with an energy dispersive X-ray spectroscopic (EDS) attachment was used for the determination of morphology and particle size of the nanomaterials. FT IR spectra of the samples are recorded using a Nicolet MAGNA-FT IR 750 spectrometer Series II.  $^1\text{H}$ ,  $^{13}\text{C}$  and  $^{31}\text{P}$  NMR experiments were carried out on a Bruker DPX-500 NMR spectrometer. UV-Vis and emission spectra of the fluorophore was measured by Cary Varian 50 scan UV-Vis optical spectrometer and Perkin Elmer LS55 Fluorescence spectrometer, respectively. The TCSPC of the fluorescent organic nanoparticle in different solvents were measured by HORIBA JOBIN YVON instrument. Morphological changes were observed with an inverted phase contrast microscope (Model: OLYMPUS IX 70, Olympus Optical Co. Ltd.).

### **Section S6: Photophysical property of TEABP**

Here we have studied various photophysical properties including UV-Vis absorption, emission spectra, solid state absorption spectra, and TCSPC measurement of TEABP in different solvents to prove the presence of intra-molecular charge transfer species (ICT) in the Vehicle controller which is very essential for the intra-molecular signal transaction by the activation of BAX protein in leukemic cell line. The UV-Vis absorption spectrum of TEABP have been shown in Figure S6. The spectra show strong absorption band in the region 240-280 nm

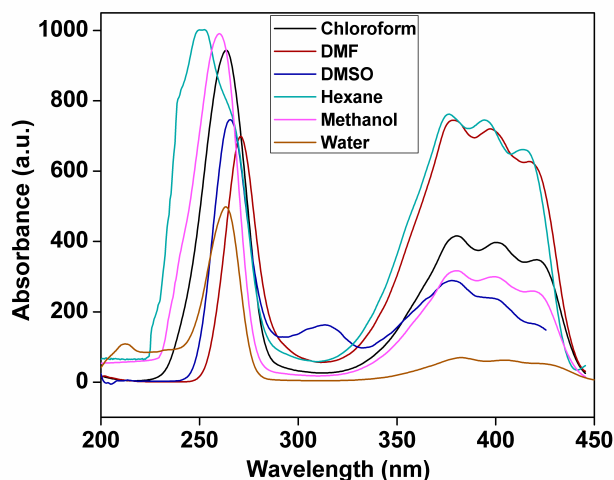


**Figure S6.** UV-Vis absorption spectra of TEABP in different solvents

corresponding to the  $\pi$ - $\pi^*$  local electron transition of the individual aromatic units and another intense absorption band in the region 375-425 nm due to the characteristic  $\pi$ - $\pi^*$  electron transition of the anthracene moiety.<sup>4</sup> Here we have used three types of solvents, nonpolar (hexane and chloroform), polar aprotic (DMF and DMSO) and polar protic (methanol and water) solvents to monitor the UV-Vis absorption and emission spectrum. For nonpolar solvents as the dielectric constant of the medium increases the  $\lambda_{\text{max}}$  in the UV-Vis spectra is red shifted indicates the greater stabilization of the excited state in relatively higher polar medium. The same trend is also followed for polar aprotic and polar protic solvents. This bathochromic shift of the absorption spectra of the TEABP with increasing polarity of the medium also indicates the greater stabilization of the excited state in polar medium.<sup>5</sup> It is expected that the red-shift is the signature of intra-molecular charge (ICT) transfer in the molecule upon excitation.<sup>6</sup>

### **Section S7: Solid state optical property of TEABP FON**

Solid state photophysical properties of the fluorescent nanoparticles are investigated in thin film on quartz substrate. The pertinent data is represented in Figure S7. The UV-Vis spectra

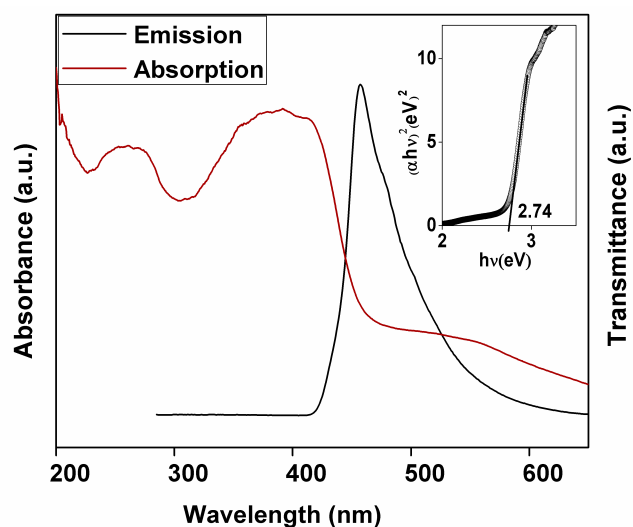


**Figure S7.** Solid state absorption and emission spectrum of TEABP and the corresponding optical band-gap between HOMO and LUMO are shown in inset show two strong absorption bands in the region 240-280 nm with maxima at 260 nm and another band at 350-415 nm with maxima at 392 nm. The optical energy band gaps of TEABP is measured to be 2.75 eV calculated from the threshold of optical absorption (415 nm) (inset of Figure S7). The corresponding emission spectra of TEABP nanoparticles are also shown in

Figure S7. The pure blue emission (450 nm) spectrum showed with very high intensity ( $2.34 \times 10^7$ ) of the solid film suggesting the minimal intermolecular interactions in the ground state of the molecule.<sup>7</sup>

### **Section S8: Emission spectrum of TEABP**

There is a large Stoke's shift in the emission maxima depending on the solvent polarity. (Fig. 4) In the nonpolar solvents (hexane, chloroform) there is two prominent emission bands but with increasing the polarity of the solvents the intensity of the peaks gradually decreases and simultaneously they lose their identity. In highly polar aqueous medium two peaks merged into a single peak with a high bathochromic shift.<sup>8</sup> This unusual emission spectrum of the molecule is probably due to the coexistence of two type of fluorophore in the excited state of the solvated medium.<sup>9</sup> One is locally excited (LE) state, generated due to the excess energy absorbed by the molecule in the optical excitation and another is intra molecular charge transfer (ICT) species, which is generated due to the pushing of highly mobile  $\pi$  electrons of the anthracene unit to the attached phosphorous with vacant  $d$  orbitals.<sup>10</sup> Now it is obvious that with increasing the polarity of the medium the stability of the ICT species will increase and simultaneously hamper the formation of locally excited species which is also reflected from the emission spectra of the molecule.<sup>11</sup> Now if we notice the emission spectrum of TEABP, there is two prominent emission peaks for TEABP in hexane (430nm, 450 nm) and chloroform (442 nm, 462 nm). The first emission peak (430 nm for hexane and 442 nm for chloroform) is probable responsibly for locally excited species and the later one (450 nm for hexane and 462 nm for chloroform) is due to the charge transfer species. In methanol, DMF and DMSO, although the two peaks are losing their identity gradually but still they are separable. But in aqueous medium the ICT species is highly stable and it is reflected from the emission spectrum, two peaks completely merged to a broad peak centered at 472 nm. The red-shift in the emission spectra of the molecule in solvents with higher polarity signifies gradually greater stabilization of ICT species in polar environment. As the dielectric constant of the solvent increases, the stability of the excited state increases and the tendency of the molecule to return its ground state decreases. As a result the fluorescence intensity of the solvated molecule decreases as the polarity of the medium increases.<sup>12</sup> From the UV-Vis absorption and emission spectroscopy it is clear that the solvent molecule affect the energy difference between the ground and excited state of the molecule (TEABP). It has been

reported in literature that Lippert-Mataga equation is suitable for measuring the solvent effect photophysics of flurophore molecule qualitatively.<sup>13</sup> To derive the Lippert-Mataga equation it has been assumed that the energy difference between the ground state and excited state of

**Table1S.** The absorption and emission wavelengths of TEABP in different solvents<sup>a</sup>

Entry	Solvent	$\epsilon$	$\Delta f(\epsilon, \eta)$	$\lambda_{\text{abs}}$ (nm)	$\lambda_{\text{emm}}$ (nm)	$\Delta v$ (cm <sup>-1</sup> ) <sup>b</sup>
1	Hexane	1.9	0.0007	250, 376, 395, 412	430, 450	2050
2	Chloroform	4.8	0.148	262, 380, 401, 420	442, 462	2164
3	Methanol	32.7	0.310	260, 381, 402, 418	446, 463	2325
4	Dimethylformamide	38.0	0.270	270, 381, 400, 417	442, 461	2288
5	Dimethyl sulfoxide	46.0	0.260	265, 380, 401, 419	444, 463	2268
6	Water	80.0	0.318	263, 383, 406, 425	472	2342

<sup>a</sup> Dielectric constants ( $\epsilon$ ) and Lippert solvent polarity parameters  $\Delta f(\epsilon, \eta)$  of different solvents are provided.

<sup>b</sup> Stoke's shifts ( $\Delta v$ ) were calculated from the difference between  $\lambda_{\text{max}}$  of the absorption and emission spectra.

molecule depends on the refractive index ( $\eta$ ) and dielectric constant ( $\epsilon$ ) of the solvent.<sup>14</sup> The equation is numerically expressed as

$$\bar{\nu}_A - \bar{\nu}_F = \frac{2}{hc} \left[ \frac{\epsilon - 1}{2\epsilon + 1} - \frac{\eta^2 - 1}{2\eta^2 + 1} \right] \frac{(\mu_E - \mu_G)^2}{a^3} + \text{constant}$$

In this equation  $\bar{\nu}_A$  and  $\bar{\nu}_F$  is the absorption and emission wave number (in cm<sup>-1</sup>) of the molecule. 'h' is the Plank's constant, 'c' is the velocity of light, 'a' is the radius of the molecule and  $\mu_E$  and  $\mu_G$  are the dipole moments of the molecule in excited and ground state respectively. The first term inside the bracket consider the effect of reorientation of solvent dipole and redistribution of electrons in the solvent molecule in the spectral change of flurophore molecule. The second term accounts for redistribution of electrons only. The difference between these two terms is known as orientation polarizability [ $\Delta f(\epsilon, \eta)$ ] and mathematically expressed as follow

$$[\Delta f(\epsilon, \eta)] = \left[ \frac{\epsilon - 1}{2\epsilon + 1} - \frac{\eta^2 - 1}{2\eta^2 + 1} \right]$$

Lippert-Mataga (L-M) plot has been constructed by plotting the Stokes shifts ( $\Delta\nu$ ) of TEABP in different solvents against corresponding orientation polarizability  $[\Delta f(\epsilon, \eta)]$ .<sup>14</sup> The linearity in the Lippert-Mataga plot corresponds that there is no specific interaction (like hydrogen bonding) and no chemical reaction between the fluorophore molecules and solvent molecules.<sup>14</sup> (Figure S8) The positive slope in the L-M plot indicates that there is a bathochromic shift due to the electronic transition from the ground state to the excited state by intramolecular charge transfer following the electron distribution in the excited state which is more polar than ground state ( $\mu_E > \mu_G$ ).<sup>15</sup> The change in the dipole moment of the molecule is around 0.56D. The molecule (TEABP) is highly symmetrical that is the reason behind very low difference in dipole moment between ground state and excited state of the molecule.<sup>16</sup> The corresponding results are listed in Table 1S.

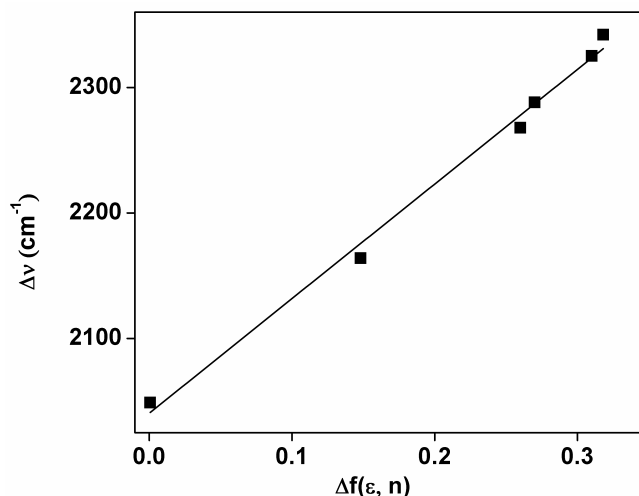


**Figure S8.** Lippert-Mataga plot; linearity in the L-M plot proves that there is no chemical interaction between the solvents and TEABP molecule

### **Section S9: ICT VS intermolecular aggregation**

The photophysical data indicates the presence of whether Intramolecular charge transfer (ICT) species or intermolecular aggregation along with locally excited (LE) state. But here we have studied the photophysical property of TEABP molecule in different solvents with concentration of  $1.04 \times 10^{-7}$  mole  $\text{dm}^{-3}$ , which is very low. Generally when the concentration of chromophore

molecule in the solvent remained below 1-10 micromolar  $\text{dm}^{-3}$  then the possibility of intermolecular aggregation is very low.<sup>17</sup> Still we have monitored the UV-Vis absorption and

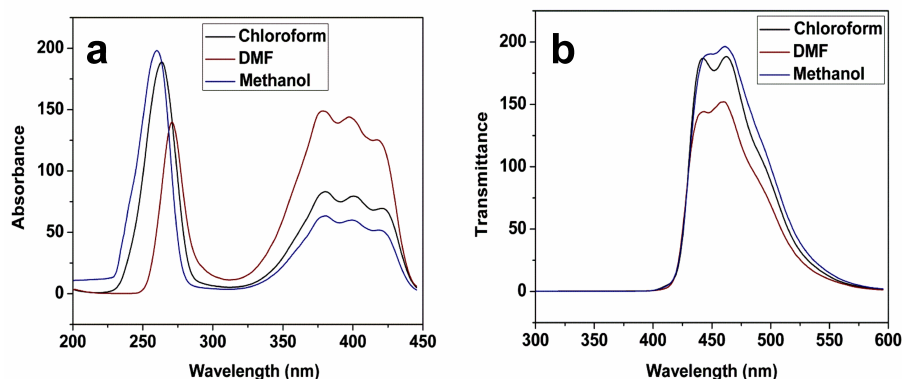


**Figure S9.** UV-Vis absorption (a) and emission (b) spectra of TEABP ( $1.04 \times 10^{-8}$  mole  $\text{dm}^{-3}$ ) in different solvents

emission spectra of the TEABP molecule in different solvents by diluting the mother solution ( $1.04 \times 10^{-7}$  mole  $\text{dm}^{-3}$ ) by 10 times but in every case the peak positions remain unaltered which signifies that the possibility of intermolecular aggregation can be ruled out. (Figure S9)

### **Section S10: FE SEM image of TEAB**

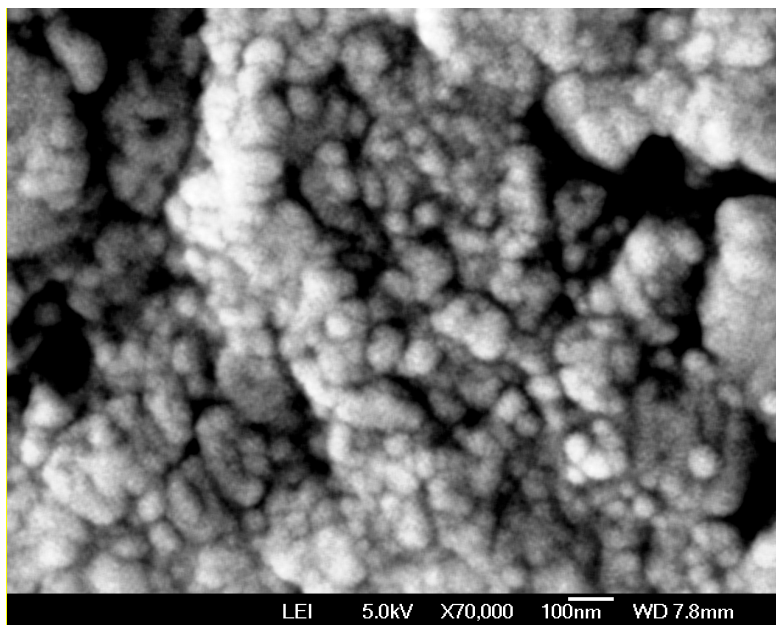


**Figure S10.** FE SMM image of TEABP

### Section S11: Time resolved spectroscopy

Room temperature time resolved emission spectra of the TEABP in different polar solvents are shown in Figure S10 and the corresponding results for non polar solvents are shown in the inset of Figure S10. For time resolved study we have used excitation wavelength 280 nm. We have

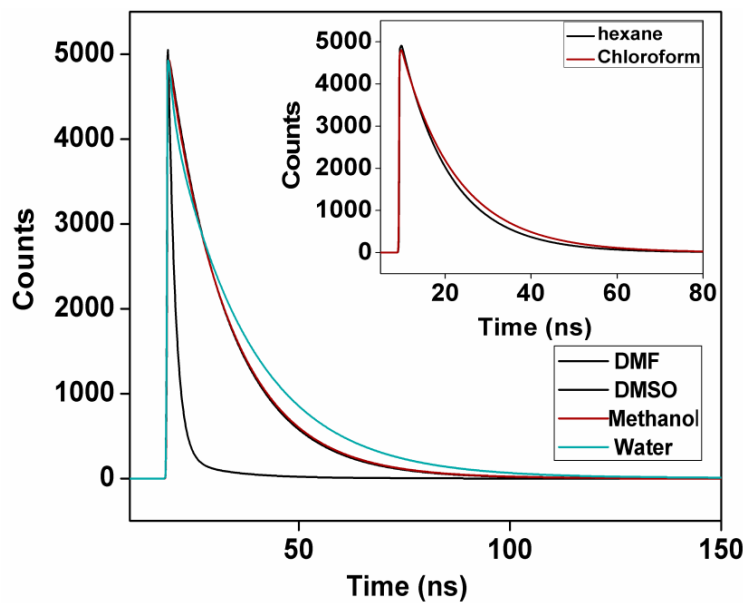


**Figure S11.** Time resolved emission spectra of TEABP in different polar solvents and the corresponding results for non-polar solvents are shown in inset.

measured the life-time of TEABP by monitoring the emission at its steady state emission wavelengths. The life-time of the different components in various solvents after fitting the decay curves are listed in Table 2S. After analyzing the results of Table 2S, we can conclude that in every solvent two excited species are formed. In hexane, for example, one species having life-time 5.98 ns with a relative abundance 3.59 % and other with a life-time 11.85 ns with a relative abundance 96.41 % have been formed. As there are two prominent peaks in the steady state emission spectra of the molecule in the nonpolar solvents we have measured the life-time of the molecule in two wavelengths (430 nm and 450 nm) but the results remain all about unaltered. In chloroform the relative abundance of the two species are 3.36 % and 96.64 % with life time 6.79 ns and 13.55 ns. For DMF, DMSO, methanol and water the relative abundance of the second

**Table2S.** The life-time of each species (in nanosecond) of TEABP in different solvents at monitoring wavelengths ( $\lambda_{\text{mon}}$ ).<sup>a</sup>

Entry	Solvent	$\lambda_{\text{mon}}$	$\tau_1$ (ns)	A1	$\tau_2$ (ns) □	A2	$\chi^2$
1	Hexane <sup>b</sup>	430	5.980	3.590	11.855	96.410	1.093
		450	6.010	3.320	11.905	96.680	1.128
2	Chloroform <sup>c</sup>	442	6.794	3.360	13.558	96.640	1.085
		462	6.613	3.250	13.637	96.750	1.035
3	Dimethylformamide	441	6.887	2.610	14.45	97.390	1.047
4	Dimethyl sulfoxide	443	0.009	19.240	12.349	80.760	1.050
5	Methanol	445	0.085	1.320	14.637	98.680	1.041
6	Water	470	1.180	1.390	18.782	98.610	1.032

<sup>a</sup> The sample was excited at 375 nm.

<sup>b,c</sup> The life-time of the species were measured at two steady state emission wavelength.

species are 97.39 %, 80.76 %, 98.68 % and 98.61 % with life time 14.45 ns, 12.34 ns, 14.63 ns and 18.78 ns respectively. So it is clear from the above discussion that the life-time and relative abundance of second specie *i.e.* charge transfer state increases as the dielectric constant of the medium increase with some discrepancy for DMSO. As in the polar solvents the life-time of the intramolecular charge transfer species is very high compare to the locally excited species the two peaks merged to a single broad peak in the steady state emission spectroscopy. But for non-polar solvents the life-time difference between the two species (LE and ICT) are moderate so two distinctly recognizable peaks arise in the emission spectra of the molecule in non-polar solvents like hexane and chloroform.<sup>18</sup>

### **Section S12: pH dependent emission study of TEABP**

To understand the charge-transfer mechanism of the molecule in the ground and excited states pH dependent absorption and emission spectra of the molecule has been taken in water at room temperature. The recorded absorption and emission spectra has been shown in Figure S11. When we add micromolar concentration of strong acid (HCl) or base (NaOH) there is no change in the

absorption spectra of the TEABP from its neutral aqueous medium. So the presence of excess  $H^+$  or  $OH^-$  does not hamper the ground state energy levels of the molecules. The emission spectra of the molecule also does not show any significant change in peak position with addition of excess  $H^+$  or  $OH^-$  but the intensity of the emission spectra hugely changed depending on the concentration of acid or base. From Figure S11 it is clear that as the concentration of  $H^+$  increases in the medium the emission intensity increases and the visa versa is also true. From this photophysical observation we have proposed a mechanism for the formation of ICT specie Scheme 1S. From the proposed mechanism, it is clear that as the concentration of  $H^+$  increases the electron draining from anthracene moiety to the adjacent phosphonate unit facilitated without

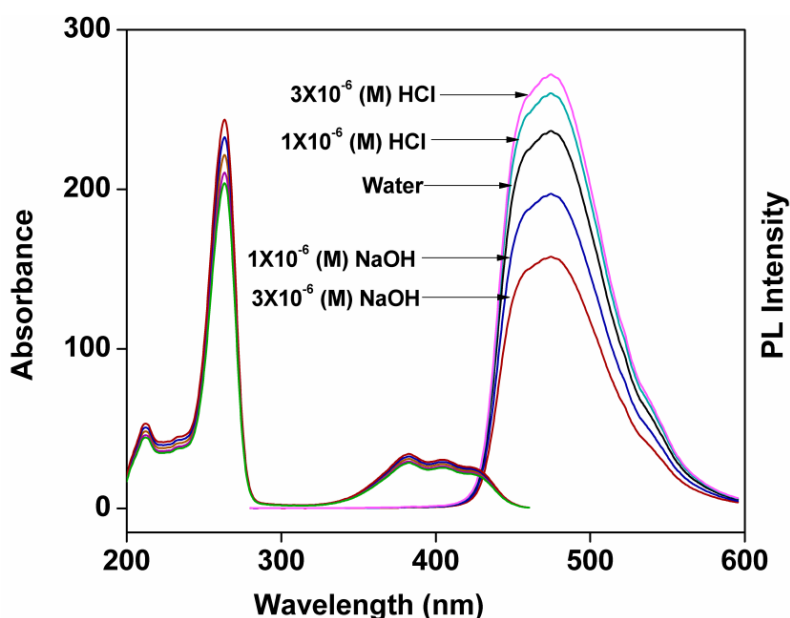
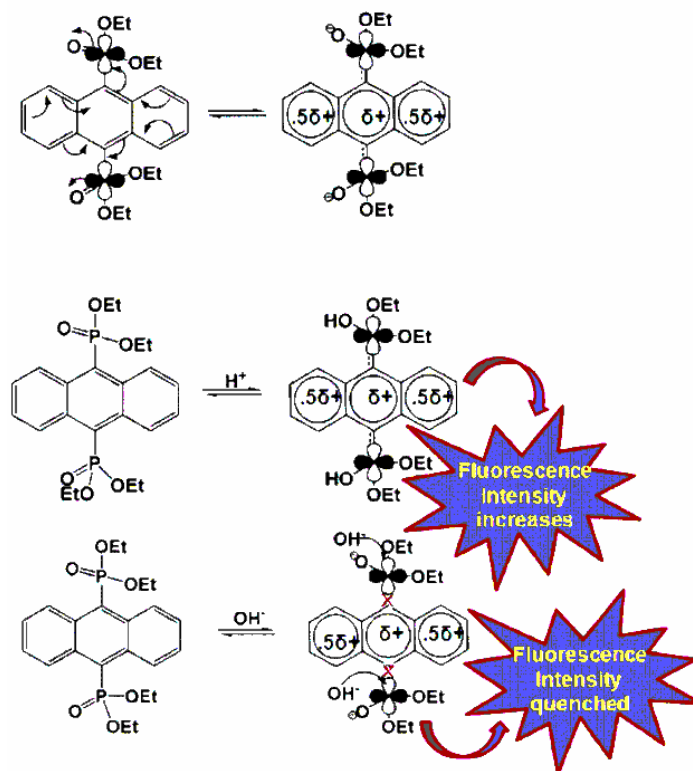


**Figure S12.** pH dependent emission spectra of TEABP

altering the chromophore length. When excess  $OH^-$  present in the medium, it acts as a nucleophile and attack to the vacant  $d$  orbital of phosphorous of the phosphonate group. Due to this phenomenon at higher pH condition the electron draining process through electron donation is hampered and it is reflected from the pH dependent emission spectra of TEABP.<sup>19</sup>



**Scheme S1.** Mechanism for pH dependent emission spectra.

### **Section S13: Emission study of TEABP FON in water**

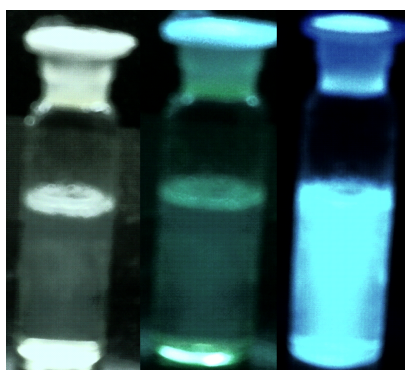


**Figure S13.** The fluorescence emission of TEABP ( $4.68 \times 10^{-5}$  mg/mL) in water under the visible light (left) and UV light with short wavelength (254 nm, middle) and long wavelength (366 nm, right)

### Section 14: Bond lengths and bond angles of minimum energy structure of TEABP

#### Bond lengths of TEABP

C(1)-C(2)	1.366
C(1)-C(6)	1.421
C(1)-H(54)	1.110
C(2)-C(3)	1.487
C(2)-H(53)	1.107
C(3)-C(4)	1.505
C(3)-H(58)	1.149
C(4)-C(5)	1.408
C(4)-C(7)	1.392
C(5)-C(6)	1.423
C(5)-C(10)	1.423
C(6)-H(56)	1.118
C(7)-C(8)	1.418
C(7)-P(16)	1.608
C(8)-C(9)	1.464
C(8)-C(11)	1.412
C(9)-C(10)	1.397
C(9)-C(14)	1.445
C(10)-P(15)	1.700
C(11)-C(12)	1.380
C(11)-H(57)	1.104
C(12)-C(13)	1.416
C(12)-H(52)	1.107
C(13)-C(14)	1.367
C(13)-H(51)	1.107
C(14)-H(55)	1.116
P(15)-O(17)	1.452
P(15)-O(18)	1.595
P(15)-O(26)	1.595
P(16)-O(34)	1.634
P(16)-O(35)	1.549
P(16)-O(43)	1.554
O(18)-C(23)	1.429
C(19)-C(23)	1.509
C(19)-H(20)	1.116
C(19)-H(21)	1.116
C(19)-H(22)	1.119
C(23)-H(24)	1.125
C(23)-H(25)	1.127

C(23)-H(25)	1.127
O(26)-C(31)	1.429
C(27)-C(31)	1.510
C(27)-H(28)	1.119
C(27)-H(29)	1.116
C(27)-H(30)	1.116
C(31)-H(32)	1.127
C(31)-H(33)	1.125
O(35)-C(40)	1.443
C(36)-C(40)	1.507
C(36)-H(37)	1.120
C(36)-H(38)	1.116
C(36)-H(39)	1.118
C(40)-H(41)	1.127
C(40)-H(42)	1.123
O(43)-C(48)	1.436
C(44)-C(48)	1.507
C(44)-H(45)	1.120
C(44)-H(46)	1.116
C(44)-H(47)	1.118
C(48)-H(49)	1.127
C(48)-H(50)	1.123
C(1)-C(2)	1.366
C(1)-C(6)	1.421
C(1)-H(54)	1.110
C(2)-C(3)	1.487
C(2)-H(53)	1.107
C(3)-C(4)	1.505
C(3)-H(58)	1.149
C(4)-C(5)	1.408
C(4)-C(7)	1.392
C(5)-C(6)	1.423
C(5)-C(10)	1.423
C(6)-H(56)	1.118
C(7)-C(8)	1.418
C(7)-P(16)	1.608
C(8)-C(9)	1.464
C(8)-C(11)	1.412

C(9)-C(10)	1.397
C(9)-C(14)	1.445
C(10)-P(15)	1.700
C(11)-C(12)	1.380
C(11)-H(57)	1.104
C(12)-C(13)	1.416
C(12)-H(52)	1.107
C(13)-C(14)	1.367
C(13)-H(51)	1.107
C(14)-H(55)	1.116
P(15)-O(17)	1.452
P(15)-O(18)	1.595
P(15)-O(26)	1.595
P(16)-O(34)	1.634
P(16)-O(35)	1.549
P(16)-O(43)	1.554
O(18)-C(23)	1.429
C(19)-C(23)	1.509
C(19)-H(20)	1.116
C(19)-H(21)	1.116
C(19)-H(22)	1.119
C(23)-H(24)	1.125
C(23)-H(25)	1.127
O(26)-C(31)	1.429
C(27)-C(31)	1.510
C(27)-H(28)	1.119
C(27)-H(29)	1.116
C(27)-H(30)	1.116
C(31)-H(32)	1.127
C(31)-H(33)	1.125
O(35)-C(40)	1.443
C(36)-C(40)	1.507
C(36)-H(37)	1.120
C(36)-H(38)	1.116
C(36)-H(39)	1.118
C(40)-H(41)	1.127
C(40)-H(42)	1.123
O(43)-C(48)	1.436

C(44)-C(48)	1.507
C(44)-H(45)	1.120

C(44)-H(46)	1.116
C(44)-H(47)	1.118

C(48)-H(49)	1.127
C(48)-H(50)	1.123

**Bond Angles of TEABP**

C(2)-C(1)-C(6)	122.484
C(2)-C(1)-H(54)	120.087
C(6)-C(1)-H(54)	117.398
C(1)-C(2)-C(3)	118.177
C(1)-C(2)-H(53)	123.686
C(3)-C(2)-H(53)	117.878
C(2)-C(3)-C(4)	112.161
C(2)-C(3)-H(58)	104.433
C(4)-C(3)-H(58)	110.055
C(3)-C(4)-C(5)	121.816
C(3)-C(4)-C(7)	113.318
C(5)-C(4)-C(7)	124.708
C(4)-C(5)-C(6)	115.783
C(4)-C(5)-C(10)	117.059
C(6)-C(5)-C(10)	126.763
C(1)-C(6)-C(5)	121.544
C(1)-C(6)-H(56)	118.835
C(5)-C(6)-H(56)	119.447
C(4)-C(7)-C(8)	117.551
C(4)-C(7)-P(16)	108.356
C(8)-C(7)-P(16)	133.871

C(7)-C(8)-C(9)	118.342
C(7)-C(8)-C(11)	122.510
C(9)-C(8)-C(11)	119.145
C(8)-C(9)-C(10)	121.326
C(8)-C(9)-C(14)	116.049
C(10)-C(9)-C(14)	122.608
C(5)-C(10)-C(9)	119.623
C(5)-C(10)-P(15)	115.820
C(9)-C(10)-P(15)	124.556
C(8)-C(11)-C(12)	122.093
C(8)-C(11)-H(57)	118.557
C(12)-C(11)-H(57)	119.348
C(11)-C(12)-C(13)	119.673
C(11)-C(12)-H(52)	120.561
C(13)-C(12)-H(52)	119.764
C(12)-C(13)-C(14)	120.275
C(12)-C(13)-H(51)	119.441
C(14)-C(13)-H(51)	120.284
C(9)-C(14)-C(13)	122.667
C(9)-C(14)-H(55)	118.381
C(13)-C(14)-H(55)	118.952

C(10)-P(15)-O(17)	117.762
C(10)-P(15)-O(18)	100.666
C(10)-P(15)-O(26)	101.356
O(17)-P(15)-O(18)	116.400
O(17)-P(15)-O(26)	116.151
O(18)-P(15)-O(26)	101.835
C(7)-P(16)-O(34)	99.538
C(7)-P(16)-O(35)	114.160
C(7)-P(16)-O(43)	118.896
O(34)-P(16)-O(35)	109.171
O(34)-P(16)-O(43)	107.955
O(35)-P(16)-O(43)	106.534
P(15)-O(18)-C(23)	118.917
H(20)-C(19)-C(23)	110.623
H(20)-C(19)-H(21)	108.526
H(20)-C(19)-H(22)	108.783
H(21)-C(19)-C(23)	111.615
H(21)-C(19)-H(22)	108.509
H(22)-C(19)-C(23)	108.721
O(18)-C(23)-C(19)	110.053
O(18)-C(23)-H(24)	108.923

O(18)-C(23)-H(25) 105.992	108.942	C(36)-C(40)-H(41) 110.791
C(19)-C(23)-H(24) 111.815	C(27)-C(31)-H(32) 110.005	C(36)-C(40)-H(42) 112.887
C(19)-C(23)-H(25) 109.952	C(27)-C(31)-H(33) 111.733	H(41)-C(40)-H(42) 110.583
H(24)-C(23)-H(25) 109.936	H(32)-C(31)-H(33) 109.908	P(16)-O(43)-C(48) 124.633
P(15)-O(26)-C(31) 118.909	P(16)-O(35)-C(40) 123.333	H(45)-C(44)-C(48) 108.683
H(28)-C(27)-C(31) 108.699	H(37)-C(36)-C(40) 108.501	H(45)-C(44)-H(46) 108.678
H(28)-C(27)-H(29) 108.417	H(37)-C(36)-H(38) 108.654	H(45)-C(44)-H(47) 108.530
H(28)-C(27)-H(30) 108.774	H(37)-C(36)-H(39) 108.581	H(46)-C(44)-C(48) 111.724
H(29)-C(27)-C(31) 111.639	H(38)-C(36)-C(40) 111.791	H(46)-C(44)-H(47) 108.698
H(29)-C(27)-H(30) 108.548	H(38)-C(36)-H(39) 108.708	H(47)-C(44)-C(48) 110.458
H(30)-C(27)-C(31) 110.695	H(39)-C(36)-C(40) 110.535	O(43)-C(48)-C(44) 109.512
O(26)-C(31)-C(27) 110.304	O(35)-C(40)-C(36) 109.158	O(43)-C(48)-H(49) 105.471
O(26)-C(31)-H(32) 105.771	O(35)-C(40)-H(41) 105.110	O(43)-C(48)-H(50) 107.460
O(26)-C(31)-H(33)	O(35)-C(40)-H(42) 107.966	

## References

1	T. Mosmann, <i>J. Immunol Methods</i> , 1983, <b>65</b> , 55–63.
2	S. Hamada and S. Fujita, <i>Histochem.</i> , 1983, <b>79</b> , 219–216.
3	J. Kern and J. P. Kehrer, <i>Chem. Biol Interact.</i> , 2002, <b>139</b> , 79–95.
4	P. Belser, R. Dux, M. Baak, L. D. Cola and V. Balzani, <i>Angew. Chem. Int. Ed</i> , 1995, <b>34</b> , 595-598.
5	V. Karunakaran, P. Ramamurthy, T. Josephrajan and V. T. Ramakrishnan, <i>Spectrochimica Acta Part A</i> , 2002, <b>58</b> , 1443-1451.
6	R. Misra, A. Mandal, M. Mukhopadhyay, D. K. Maity and S. P. Bhattacharyya, <i>J. Phys. Chem. B</i> , 2009, <b>113</b> , 10779-10791.
7	S. Tao, S. Xu and X. Zhang, <i>Chem. Phys. Lett.</i> , 2006, <b>429</b> , 622-627.

8	(a) D. C. Khara and A. Samanta, <i>J. Phys. Chem. B</i> , 2012, <b>116</b> , 13430-13438; (b) K. Kalyanasundaram, J. K. Thomas, <i>J. Phys. Chem.</i> , 1977, <b>81</b> , 2176-2180.
9	A. Demeter and T. Berces, <i>J. Phys. Chem. A</i> , 2001, <b>105</b> , 4611-4621.
10	J. C. Duchamp, M. Pakulski, A. H. Cowley and K. W. Zilm, <i>J. Am. Chem. Soc.</i> , 1990, <b>112</b> , 6803-6809
11	R. E. Ellis, J. Y. Yuan and H. R. Horvitz, <i>Annu Rev Cell Bio.</i> , 1991, <b>7</b> , 663-698.
12	S. Hashimoto, <i>J. Phys. Chem.</i> , 1993, <b>97</b> , 3662-3667.
13	R. Nandy and S. Sankararaman, <i>Beilstein J. Org. Chem.</i> , 2010, <b>6</b> , 992-1001.
14	J. R. Lakowicz, Principles of Fluorescence Spectroscopy, 3rd Ed., Springer, New York, <b>2006</b> .
15	Y. Ooyama, G. Ito, K. Kushimoto, K. Komaguchi, I. Imae and Y. Harima, <i>Org. Biomol. Chem.</i> , 2010, <b>8</b> , 2756-2770.
16	G. F. Mes, B. D. Jong, H. J. V. Ramesdonk, J. W. Verhoeven, J. M. Warman, M. P. D. Haas and L. E. W. H. D. Dool, <i>J. Am. Chem. Soc.</i> , 1984, <b>106</b> , 6524-6528.
17	X. Dai, M. E. Eccleston, Z. Yue, N. K.H. Slater and C. F. Kaminski, <i>Polymer</i> , 2006, <b>47</b> , 2689-2698.
18	(a) M. A. Izquierdo, T. D. M. Bell, S. Habuchi, E. Fron, R. Pilot, T. Vosch, S. D. Feyter, J. Verhoeven, J. Jaco, K. Mullen, J. Hofkens and F. C. D. Schryver, <i>Chem. Phys. Lett.</i> , 2005, <b>401</b> , 503-508; (b) D. Chandra, A. Dutta and A. Bhaumik, <i>Eur. J. Inorg. Chem.</i> , 2009, 4062-4068.
19	(a) D. Li, J. Song, P. Yin, S. Simotwo, A. J. Bassler, Y. Aung, J. E. Roberts, K. I. Hardcastle, C. L. Hill and T. Liu, <i>J. Am. Chem. Soc.</i> , <b>2011</b> , <i>133</i> , 14010-14016; (b) D. J. Peterson and H. R. Hays, <i>J. Org. Chem.</i> , <b>1965</b> , <i>30</i> , 1939-1942.